JOINT INSTITUTE FOR NUCLEAR RESEARCH

Laboratory of Radiation Biology

FINAL REPORT ON THE INTEREST PROGRAMME

Analysis of Water Radiolysis Under Different LET and Oxygen Conditions Using TOPAS-nBio

Supervisor:
Dr. Ivan Padron Diaz

Student:
Thalia Rodriguez Martinez, University of Havana

Participation period:
02 March - 19 April, Wave 14

Dubna, 2026

Abstract

This study investigates the influence of Linear Energy Transfer (LET) and oxygen concentration on water radiolysis using Monte Carlo simulations with TOPAS-nBio. Two radiation types were analyzed: low-LET 4 keV electrons and high-LET 4 MeV alpha particles. The chemical evolution of key radiolytic species was evaluated through time-dependent G-values under varying oxygen conditions (0–250 µM). Results show that low-LET radiation produces higher yields of reactive radicals such as •OH and hydrated electrons, with strong sensitivity to oxygen, leading to significant depletion of e_{aq}^- and H•. In contrast, high-LET radiation promotes intra-track recombination, resulting in lower radical yields and enhanced production of molecular species like H_2O_2, with reduced oxygen dependence. The findings provide a quantitative comparison of LET effects through the $G(e^-)/G(\alpha)$ ratio and offer insight into radiobiological phenomena such as the Oxygen Enhancement Ratio (OER) and the FLASH effect. These results highlight the critical role of radiation quality in indirect damage mechanisms.

1. Introduction

1.1 Water radiolysis as an indirect damage mechanism

When ionizing radiation interacts with biological matter, a large fraction of the damage does not occur through direct interaction with DNA, but rather through the radiolysis of water. Since water is the main constituent of biological tissues, its radiolysis leads to the formation of reactive chemical species that can subsequently induce biological damage.

The radiolysis of water involves a series of physical, physicochemical, and chemical stages that result in the production of highly reactive species such as hydroxyl radicals (•OH), hydrated electrons (e_aq^-), and hydrogen peroxide (H_2O_2) **[9]**. Among these, the hydroxyl radical is considered one of the most important agents of indirect damage due to its strong oxidizing nature **[1] [2]**. These species diffuse through the medium and interact with biomolecules, contributing significantly to radiation-induced damage.

Monte Carlo simulations have been widely used to study these processes at the microscopic level, allowing the analysis of radiation track structure and the spatial distribution of reactive species **[3]**. In this context, understanding how different types of radiation modify the chemical yields in water is essential for interpreting radiation effects in biological systems.

1.2 Linear Energy Transfer (LET) as a key variable

One of the most important parameters governing radiation-induced chemistry is the Linear Energy Transfer (LET), defined as the energy deposited per unit length along the particle track. LET strongly depends on the type, charge, and energy of the incident particle.

Low-mass particles such as electrons are characterized by low LET radiation, producing sparse ionizations along their tracks. In contrast, charged particles such as alpha particles exhibit high LET, leading to dense ionization patterns and highly localized energy deposition **[4]**.

These differences in track structure have direct consequences on the radiolysis of water. Low LET radiation tends to produce more spatially separated radicals, allowing them to diffuse and react with surrounding molecules, including dissolved oxygen. On the other hand, high LET radiation promotes recombination processes due to the high local concentration of species, reducing their effective diffusion and altering the overall chemical yields.

1.3 Reference LET values for the studied particles

For the purpose of this study, representative LET values in water were taken from the literature to characterize the radiation quality of the incident particles.

- Electrons with an energy of 4 keV are considered low LET radiation, with typical values in the range of 7–10 keV/µm **[6]**.
- Alpha particles with an energy of 4 MeV correspond to high LET radiation, with values around 120–150 keV/µm **[5]**.

These values highlight the significant difference in energy deposition density between both types of radiation.

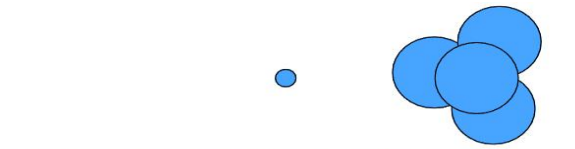

Property	Electrons	Alphas
Incident Energy	4 keV	4 MeV
Particle Type	Light (e^-)	Heavy (α)
Charge	-1	2
LET (keV/µm)	7–10	120–150
Radiation Type	Low LET	High LET
Energy Distribution	Sparse	Dense

Figure 1. Comparison between low-LET (electrons) and high-LET (alpha particles) radiation in water

1.4 Motivation of the study

Based on these differences, an important question arises: how does LET influence the chemical evolution of water following irradiation? Previous studies have shown that high LET radiation can significantly modify early chemical processes, including enhanced recombination, local pH variations, and oxygen depletion effects **[7]**. In contrast, low LET radiation tends to produce chemical species that are more sensitive to environmental conditions, particularly the presence of dissolved oxygen.

Therefore, the main motivation of this work is to analyze how the difference in LET between electrons (low LET) and alpha particles (high LET) affects the radiolysis of water, with special emphasis on the production of chemical species (G-values) and their dependence on oxygen concentration. This analysis provides insight into the role of radiation quality in indirect damage mechanisms and its potential implications in radiobiology.

2. Methodology

2.1 Simulation framework: TOPAS-nBio

All simulations were performed using TOPAS-nBio version 4.0.1 [8], a Monte Carlo track-structure simulation platform built on top of TOPAS [9] and Geant4-DNA [10]. TOPAS-nBio enables the simulation of the full water radiolysis process, from the initial physical interactions to the chemical evolution of reactive species over time. The framework models three distinct temporal stages: the physical stage (10^{-1} s), in which ionizations and excitations are produced; the pre-chemical stage (10^{-12} s), where dissociation and thermalization of water molecules occur; and the chemical stage (up to 10^{-} s), during which the chemical species diffuse and react with each other.

The physical processes were simulated using the TsEmDNAPhysics module, which implements the Geant4-DNA models for low-energy interactions in liquid water. For electron transport, the ELSEPA model was used for elastic scattering, and the Meesungnoen model was applied for the thermalization of solvated electrons [11]. The chemistry was activated through the TsEmDNAChemistry module, and the chemical evolution was computed using the Independent Reaction Times (IRT) method, which offers a computationally efficient alternative to step-by-step Brownian dynamics simulations while maintaining accuracy in the calculation of chemical yields [12].

2.2 Simulation geometry and particle sources

The simulation geometry consisted of a spherical water phantom of radius 0.5 µm, filled with liquid water (G4_WATER), placed inside an air-filled world volume of 10 µm half-length on each side. The sphere

was centered at z = 1.5 µm, and the particle beam was directed along the positive z-axis from a position at z = 0.5 µm, ensuring full irradiation of the target volume. The scoring volume coincided with the spherical water phantom.

Two types of monoenergetic particle beams were simulated to cover a wide range of LET values. First, electrons with a kinetic energy of 4 keV, representing low-LET radiation (LET ≈ 7–10 keV/µm). Second, alpha particles with a kinetic energy of 4 MeV, representing high-LET radiation (LET ≈ 120–150 keV/µm). This combination allows a direct comparison of the radiochemical response of water under very different track structure conditions.

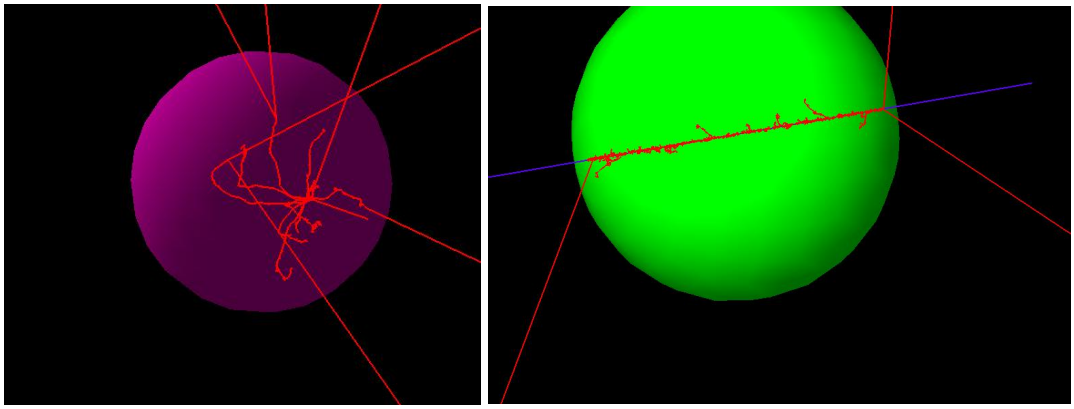

Figure 2. Particle tracks in a water sphere for different radiation types. The left image corresponds to electron irradiation (4 keV), showing sparse and extended tracks characteristic of low-LET radiation. The right image corresponds to alpha particle irradiation (4 MeV), exhibiting dense and localized tracks typical of high-LET radiation. The difference in sphere color is only for visualization purposes and does not represent any physical difference in the medium.

As shown in Figure 2, electron tracks are more spatially dispersed, while alpha particles produce dense ionization clusters. This difference reflects the contrast between low and high LET radiation and explains the variations observed in the chemical yields.

2.3 Chemical reactions and oxygen concentrations

The default set of water radiolysis reactions from the TOPAS-nBio library was used as a baseline, comprising ten bimolecular reactions between the primary radiolytic species: solvated electrons (e^-_{aq}), hydroxyl radicals (•OH), hydrogen radicals (H•), hydronium ions (H_3O^+), hydrogen peroxide (H_2O_2), molecular hydrogen (H_2), and hydroxide ions (OH^-). Reaction rates were taken from the Buxton compilation and diffusion coefficients from Plante et al. (2017) [13].
To investigate the effect of dissolved oxygen, two additional background reactions were incorporated into the chemistry configuration, following the syntax verified in the official TOPAS-nBio Fricke dosimeter example:

$$R11:\ e^-_{aq} + O_2 \rightarrow O_2^{\bullet -} \qquad (k = 1.9 \times 10^1\ M^{-1}s^{-1})$$
$$R12:\ H^\bullet + O_2 \rightarrow HO_2^\bullet \qquad (k = 2.1 \times 10^1\ M^{-1}s^{-1})$$

Reaction R12, in which the hydrogen radical reacts with molecular oxygen to form the hydroperoxyl radical (HO_2•), is considered the most radiobiologically relevant due to its high rate and its role in redirecting H• away from recombination pathways. Both reactions were implemented as background reactions with a fixed initial oxygen concentration, representing dissolved O_2 uniformly distributed in the water volume prior to irradiation. Reaction rates were taken from the Buxton et al. compilation [13].
Four initial oxygen concentrations were simulated for each particle type, selected to represent physiologically relevant oxygenation levels found in biological tissues **[8]**:

- 0 µM — pure water without dissolved oxygen (baseline condition)
- 10 µM — representative of hypoxic tumor tissue (~1% O_2)
- 50 µM — representative of moderately hypoxic tissue (~5% O_2)

- 250 µM — representative of normoxic healthy tissue (~20% O_2)

These concentrations were selected based on physiological data reported in the literature for tumor and normal tissue oxygenation levels [14, 15], covering the range from severe hypoxia to full normoxia. In total, eight simulation conditions were evaluated (two particle types × four oxygen concentrations), each producing a complete set of time-dependent G-values from 1 ps to 1 µs.

2.4 G-value as the main observable

The primary observable used in this study is the G-value, defined as the number of chemical species produced or consumed per 100 eV of energy deposited in the medium. G-values were scored using the TsIRTGvalue scorer implemented in TOPAS-nBio, which computes chemical yields as a function of time using the IRT method.
To quantify the sensitivity of the radiolytic chemistry to oxygen concentration, the relative change in G-value between the anoxic (0 µM) and normoxic (250 µM) conditions was calculated for each species as:

$$\Delta G\ (\%) = |G(0\ \mu M) - G(250\ \mu M)| \,/\, G(0\ \mu M) \times 100$$

Additionally, to directly compare the effect of LET on the chemical yields, the ratio $G(e^-)/G(\alpha)$ was computed for each species and each oxygen concentration. A ratio greater than unity indicates that the low-LET electron produces a higher yield of that species, while a ratio below unity indicates the opposite. This metric enables a quantitative assessment of how radiation quality modulates the radiolytic chemistry as a function of oxygen availability, which is the central question of this study.

3. Results

3.1 Water radiolysis by 4 keV electrons (low LET)

Figure 3 shows the time-dependent G-values for all chemical species produced by 4 keV electrons in pure water (0 µM O_2), spanning from 1 ps to 1 µs. At early times (t = 1 ps), the dominant species are the hydroxyl radical ($G(\bullet OH) \approx 5.1$) and the hydronium ion ($G(H_3O^+) \approx 4.1$), both produced directly from the ionization and dissociation of water molecules. The hydrated electron ($G(e^-_{aq}) \approx 4.1$) is also prominent at early times. As the simulation evolves, radical recombination and neutralization reactions progressively reduce these yields. By t = 1 µs, $G(\bullet OH)$ decreases to approximately 1.5, $G(e^-_{aq})$ to 1.5, and $G(H_3O^+)$ to 2.1, while stable products such as H_2O_2 ($G \approx 0.95$) and molecular hydrogen H_2 accumulate over time. These results are consistent with values reported in the literature for low-LET water radiolysis [3].

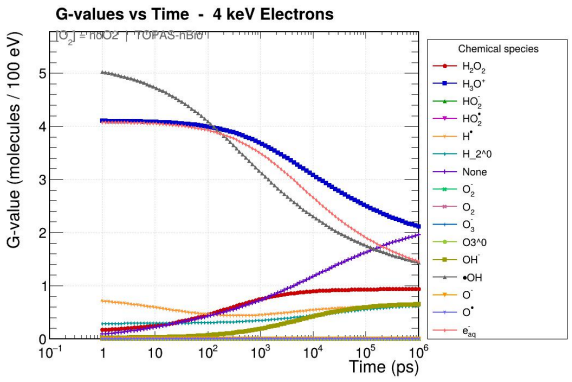

Figure 3. G-values vs Time — 4 keV Electrons, 0 µM O_2

The introduction of dissolved oxygen progressively modifies the chemical evolution of the system (Figure 4, corresponding to $[O_2]_0$ = 10, 50, and 250 µM). The most notable change is the appearance of the hydroperoxyl radical (HO_2•) as a new species exclusively produced through reaction R12 (H• + O_2 → HO_2•). Its yield increases monotonically with oxygen concentration, reaching $G(HO_2•) \approx 0.6$ at 250 µM. Simultaneously, the hydrated electron and hydrogen radical, both highly reactive with O_2, are substantially depleted already at the lowest oxygen concentration tested (10 µM), with their final yields approaching zero by 250 µM.

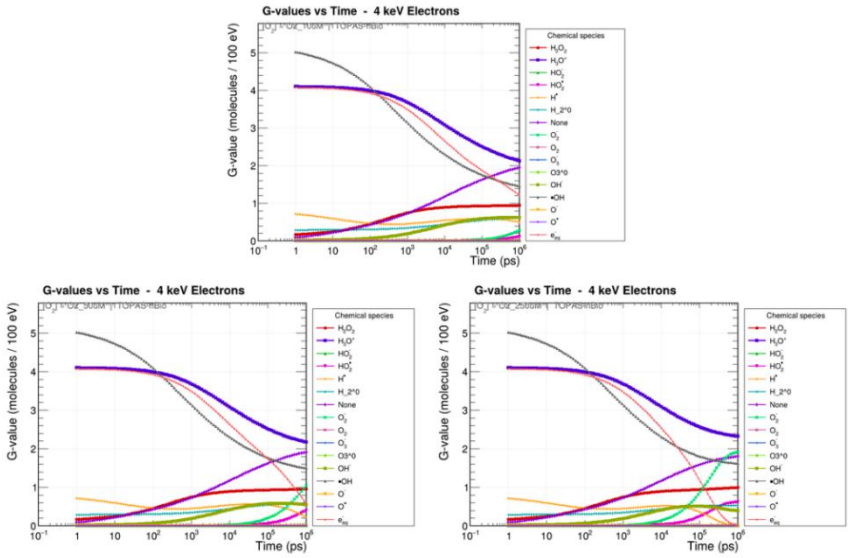

Figures 4. G-values vs Time — 4 keV Electrons at 10, 50, and 250 µM O_2

Figure 5 summarizes the oxygen dependence by showing the final G-values (at t = 1 µs) as a function of initial oxygen concentration for the key species. The most dramatic response is observed for e^-_{aq} and H•, whose yields drop from approximately 1.5 and 0.6, respectively, at 0 µM to nearly zero at 250 µM. This steep decline occurs primarily between 0 and 10 µM, indicating that the oxygen-driven capture reactions become dominant even at very low oxygen levels. In contrast, •OH shows a modest increase of approximately 12% over the same range, consistent with the reduced consumption by e^-_{aq} (reaction R4). H_2O_2 remains largely unchanged (~6% variation), while HO_2• rises from zero to ~0.6.

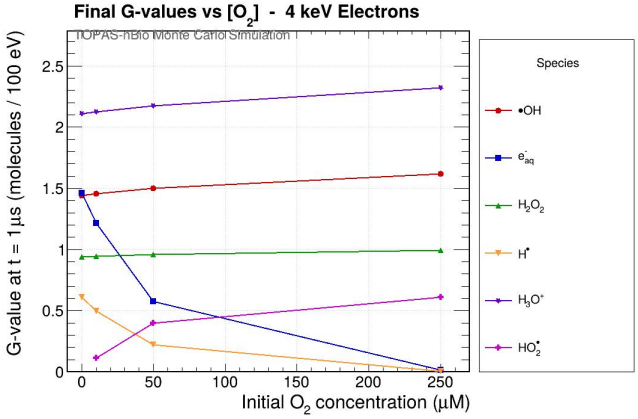

Figures 5. G-values vs Time — 4 keV Electrons at 10, 50, and 250 µM O_2

Figure 6 shows the relative change ΔG(%) between the anoxic and normoxic conditions for each species. The largest effects correspond to e^-_{aq} (99.1%) and H• (99.4%), confirming that these species are almost completely scavenged by oxygen. The •OH radical shows a moderate increase (12.0%),

while H_2O_2 (5.8%) and H_3O^+ (9.9%) exhibit smaller but non-negligible variations. These results establish the oxygen sensitivity baseline for low-LET radiation.

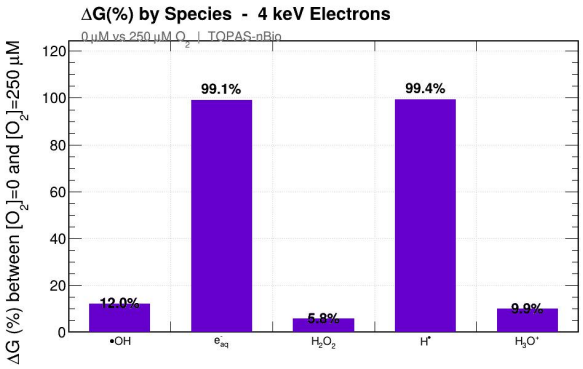

Figure 6. ΔG(%) by Species — 4 keV Electrons

3.2 Water radiolysis by 4 MeV alpha particles (high LET)

Figure 7 shows the G-value evolution for 4 MeV alpha particles in pure water. Compared to electrons, several important differences are immediately apparent. First, the temporal dynamics are shifted significantly toward later times: while for electrons the transition between radical-dominated and stable-product-dominated chemistry occurs around 10^2–10^3 ps, for alpha particles this transition takes place between 10^3 and 10 ps. This delay reflects the higher local radical density produced by the dense alpha particle track, which slows down the diffusion-limited recombination processes. Second, the final G-values for •OH, e^-_{aq}, and H• are considerably lower than for electrons (approximately 0.27, 0.10, and 0.27, respectively at t = 1 ps), confirming the well-known enhanced intra-track recombination associated with high-LET radiation. Third, H_2O_2 reaches a higher absolute yield (G ≈ 1.15) and shows a dominant role among the final products, consistent with the greater recombination of •OH radicals within the dense track core.

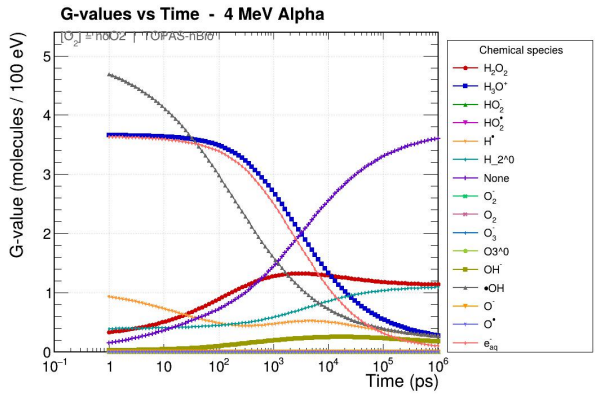

Figure 7. G-values vs Time — 4 MeV Alpha Particles, 0 µM O_2

The addition of dissolved oxygen (Figures 8, for 10, 50, and 250 µM) introduces qualitatively similar changes as observed for electrons: the appearance of HO_2•, depletion of e^-_{aq} and H•, and a slight increase in •OH. However, the magnitude of these changes and the temporal evolution differ from the low-LET case, as discussed in Section 4.

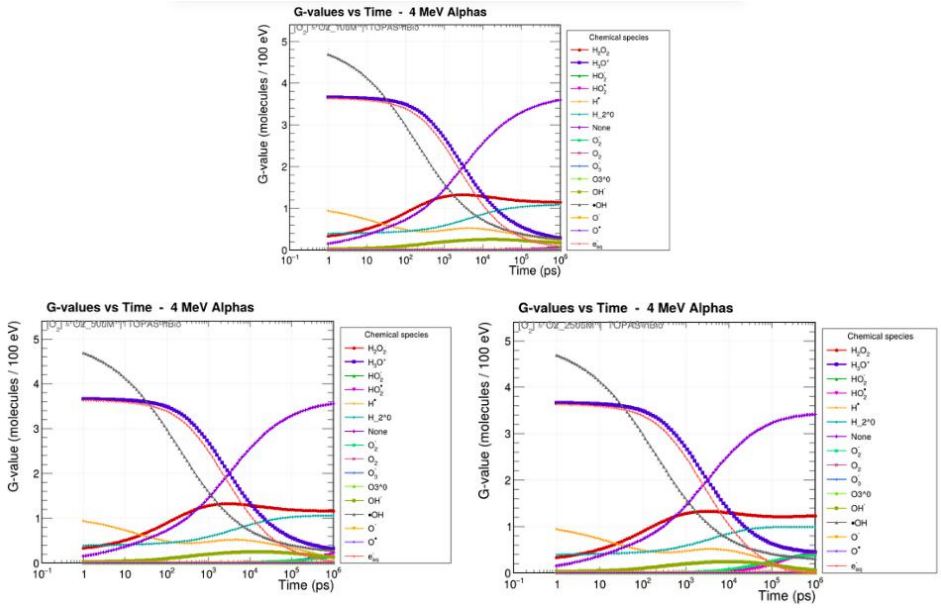

Figures 8. G-values vs Time — 4 MeV Alphas at 10, 50, and 250 μM O_2

Figure 9 shows the final G-values as a function of $[O_2]_0$ for alpha particles. The e^-_{aq} and H• yields also approach zero with increasing oxygen. Notably, H_2O_2 remains the dominant species across all oxygen concentrations (G ≈ 1.15–1.24), which contrasts with the electron case where H_2O_2 was a secondary product. The •OH radical shows a modest increase (15.4%) and HO_2• appears but reaches lower absolute values (~0.4) compared to the electron case. The H_3O^+ ion shows a pronounced relative increase of 60.0%, suggesting that the acid-base balance of the irradiated medium is more strongly affected by oxygen in the high-LET case.

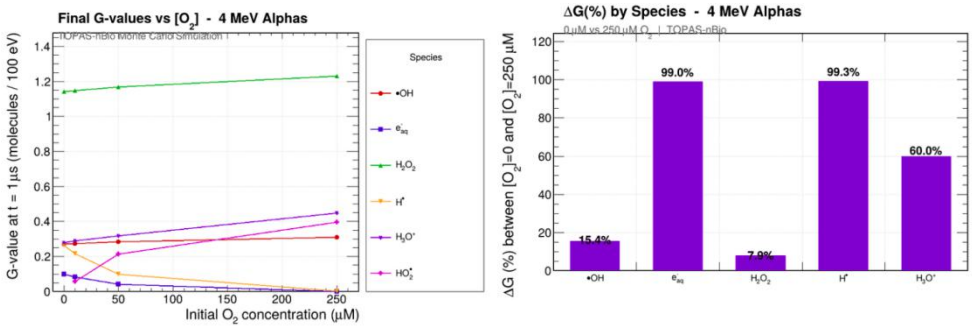

Figures 9. Final G-values vs [O_2] and ΔG(%) — 4 MeV Alphas

4. Discussion of the results

4.1 Common response to oxygen: species dominated by fast reactions

A striking finding of this study is that the hydrated electron and the hydrogen radical show nearly identical oxygen sensitivity for both particle types, with ΔG(%) values close to 99% in both cases. This result can be understood by considering the reaction kinetics: both R11 (e^-_{aq} + O_2, k = 1.9 × 10^1 $M^{-1}s^{-1}$) and R12 (H• + O_2, k = 2.1 × 10^1 $M^{-1}s^{-1}$) have rate constants among the highest in the water radiolysis system. At physiologically relevant oxygen concentrations (10–250 μM), these reactions proceed so rapidly that they are essentially complete within the first nanoseconds of the chemical stage,

before inter-radical recombination can compete. Consequently, the LET-dependent track structure does not have sufficient time to influence the fate of these two species with respect to oxygen scavenging.

4.2 LET-dependent differences: hydroxyl radical and stable products

Despite the similar behavior of e^-_{au} and H•, important LET-dependent differences emerge for other species. The absolute G-values across all conditions are substantially lower for alpha particles than for electrons, reflecting the dominant role of intra-track recombination in high-LET radiation. For •OH at 0 μM, G(•OH, e^-) ≈ 1.47 compared to G(•OH, α) ≈ 0.27 at t = 1 μs, a ratio of approximately 5.4. This difference is a direct consequence of the dense alpha track, in which a large fraction of the •OH radicals recombine with each other (reaction R10: •OH + •OH → H_2O_2) before they can escape the track. This explains why H_2O_2 is the dominant product for alpha particles across all oxygen conditions.
The H_3O^+ ion shows a particularly interesting LET-dependent response to oxygen. While the relative change is only 9.9% for electrons, it reaches 60.0% for alpha particles. This result suggests that in the high-LET case, the conversion of H• to HO_2• via reaction R12 has a more pronounced effect on the local acid-base balance, likely because the high radical density in the alpha track amplifies the proton-donation capacity of the newly formed HO_2• species. This observation is qualitatively consistent with recent reports of transient local acidification under high dose-rate and high-LET conditions [7].

4.3 The G(e^-)/G(α) ratio as a measure of LET modulation

The ratio G(e^-)/G(α) provides a compact and informative measure of how radiation quality modulates chemical yields as a function of oxygen concentration. A ratio equal to unity indicates no dependence on LET, while deviations from unity quantify the extent of LET-induced differences. Figure 10 presents this ratio for the main radiolytic species over the studied oxygen range.

For •OH, the ratio remains relatively stable around ~5.2–5.4 across all oxygen concentrations, indicating a strong and persistent LET dependence. This suggests that hydroxyl radical production is significantly higher for low-LET radiation (electrons) compared to high-LET radiation (alpha particles), and only weakly affected by oxygen. In contrast, for H_2O_2 the ratio is consistently below unity (~0.80–0.82), meaning that alpha particles produce more hydrogen peroxide than electrons. This behavior is consistent with the enhanced intra-track recombination of •OH radicals in the dense tracks of high-LET radiation, which favors molecular product formation.

For the hydrated electron (e^-_{aq}), the ratio is large (~14–15) and shows only a slight decrease with increasing oxygen concentration. This indicates that electrons produce significantly more solvated electrons than alpha particles, while oxygen acts as a scavenger that slightly reduces this difference. A clearer oxygen dependence is observed for H•, H_3O^+, and HO_2•. In these cases, the ratio decreases with increasing [O_2], for example from ~2.3 to ~2.0 for H•, from ~7.5 to ~5.2 for H_3O^+, and from ~2.0 to ~1.55 for HO_2•. This trend suggests that oxygen progressively reduces the differences between low- and high-LET radiation for species involved in oxygen-driven reaction pathways.

Overall, these results indicate that oxygen tends to partially homogenize the chemical response between radiation types, particularly for species directly involved in oxygen-related reactions. However, a clear LET dependence remains for key radicals such as •OH and e^-_{aq}, highlighting the persistent influence of track structure on water radiolysis.

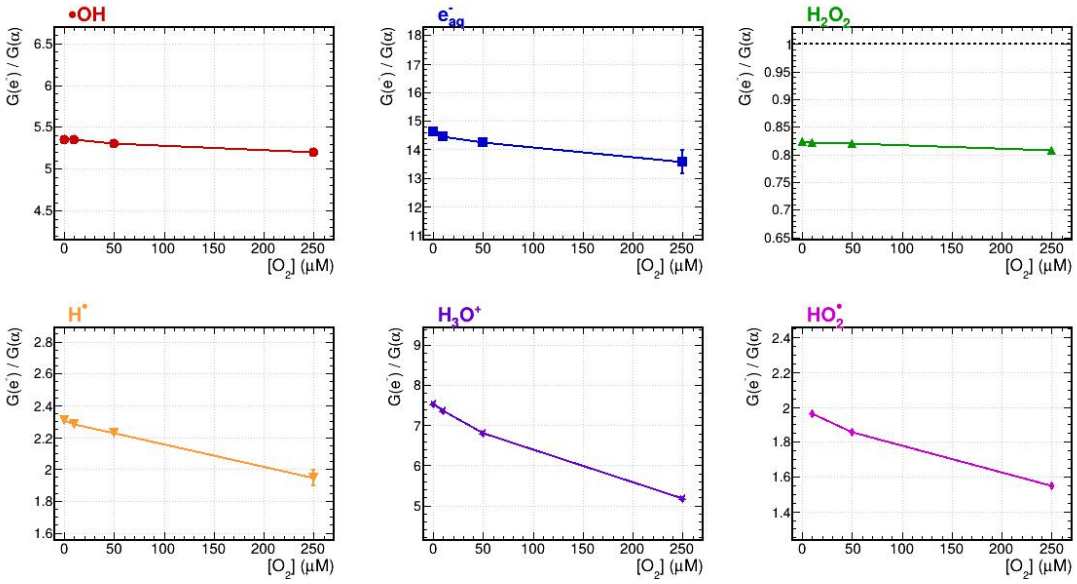

Figure 10. Ratio G(e⁻)/G(α) as a function of initial oxygen concentration for the main radiolytic species. Values above unity indicate higher yields for electron irradiation (low LET), while values below unity indicate higher yields for alpha particles (high LET).

5. Implications for OER and FLASH

5.1 Connection with Oxygen Enhancement Ratio (OER)

The observed trends can be qualitatively related to the concept of the Oxygen Enhancement Ratio (OER), which describes the increased biological effectiveness of radiation in the presence of oxygen **[10]**. It is well established that low-LET radiation exhibits a higher OER, while high-LET radiation shows a reduced oxygen effect.

The results obtained in this work are consistent with this behavior. For low-LET electrons, the strong depletion of e^-_{aq} and H• in the presence of oxygen, together with the increased formation of oxygen-derived species such as HO_2•, indicates a high sensitivity to oxygen. In contrast, for high-LET alpha particles, the dense track structure leads to enhanced radical recombination, reducing the availability of species that can interact with oxygen.

This reduced chemical sensitivity to oxygen for alpha particles provides a mechanistic explanation for the lower OER observed in high-LET radiation, where biological damage becomes less dependent on oxygen availability.

5.2 Implications for the FLASH effect

The results also provide insight into the possible chemical basis of the FLASH effect, in which ultra-high dose rate irradiation leads to reduced normal tissue toxicity. One of the proposed mechanisms for this effect is the rapid depletion of oxygen during irradiation, leading to a transient hypoxic state.

In the present results, oxygen is shown to strongly influence the yields of key reactive species, particularly for low-LET radiation. This suggests that under FLASH conditions, where oxygen

depletion may occur on very short timescales, the chemical stage of water radiolysis could be significantly altered.

In contrast, the reduced sensitivity to oxygen observed for high-LET radiation suggests that the FLASH effect may be less pronounced for particles such as alphas. This is consistent with the idea that high-LET radiation is less dependent on oxygen-mediated chemical pathways.

5.3 Limitations of the simulation

One important limitation of the present study is related to the transport of high-LET particles in the simulation framework. In particular, the parameter *MaximumNumberOfSteps* may impose constraints on the spatial resolution of alpha particle tracks, potentially affecting the accuracy of the energy deposition pattern.

Since high-LET radiation is highly sensitive to local track structure, any limitation in the step size or interaction modeling may influence the calculated chemical yields. Therefore, the results obtained for alpha particles should be interpreted with caution, especially when comparing absolute values.

7. Conclusions and future work

In this work, the effect of radiation quality (LET) and oxygen concentration on the radiolysis of water was investigated using Monte Carlo simulations with TOPAS-nBio. A clear distinction was observed between low-LET electrons and high-LET alpha particles in terms of both absolute chemical yields and their dependence on oxygen.

Low-LET radiation was found to produce higher yields of reactive radicals such as •OH and e^-_{aq}, with a strong sensitivity to oxygen concentration. In contrast, high-LET radiation exhibited lower radical yields and enhanced formation of molecular products such as H_2O_2, reflecting the dominant role of intra-track recombination.

These findings are consistent with the known behavior of the Oxygen Enhancement Ratio (OER), providing a chemical-level interpretation of the reduced oxygen effect in high-LET radiation.

As future work, it would be of great interest to extend this study to ultra-high dose rate conditions in order to simulate FLASH irradiation. In such conditions, the rapid depletion of oxygen could significantly alter the radiolytic chemistry, particularly for low-LET radiation. A direct comparison between conventional (CONV) and FLASH regimes would allow a deeper understanding of the role of oxygen in radiation-induced damage and its potential implications for radiotherapy.

Reference

[1] Spinks, J. W. T., & Woods, R. J. (1990). *An Introduction to Radiation Chemistry*. Wiley.

[2] LaVerne, J. A. (2000). OH radicals and oxidizing products in the radiolysis of water. *Journal of Physical Chemistry B*, 104(40), 10288–10294.

[3] Nikjoo, H., Uehara, S., Emfietzoglou, D., et al. (2006). Monte Carlo simulation of water radiolysis for low-energy charged particles. *Journal of Radiation Research*, 47(1), 69–81.

[4] Pimblott, S. M., & LaVerne, J. A. (2007). Effects of Linear Energy Transfer on Radiation-Induced Chemical Development of DNA. *Radiation Research*, 167(3), 283–289.

[5] Reeves, K. G., Yao, Y., & Kanai, Y. (2016). Electronic stopping power in liquid water for protons and α-particles from first principles. *Physical Review B*, 94(4), 041108.

[6] Issa, K., Almoustapha, A., & Manga Adamou, O. (2023). Collision of Incident Electrons with Liquid Water Molecules: Study of Linear Energy Transfer (LET). *Asian Journal of Physical and Chemical Sciences*, 11(4).

[7] Bepari, M. I., Meesungnoen, J., & Jay-Gerin, J.-P. (2023). Early and transient formation of highly acidic pH spikes in water radiolysis under the combined effect of high dose rate and high linear energy transfer. *Radiation*, 3(3), 165–182.

[8] McKeown SR. Defining normoxia, physoxia and hypoxia in tumours—implications for treatment response. Br J Radiol 2014;87:20130676

[9] Jay-Gerin, J.-P. Fundamentals of Water Radiolysis.Encyclopedia 2025, 5, 38. https://doi.org/10.3390/encyclopedia5010038

[10] Baatout, S. (Ed.). (2023). *Radiobiology Textbook*. Springer.
https://doi.org/10.1007/978-3-031-18810-7 (doi.org in Bing)